PERGAMON

AVAILABLE AT
www.ComputerScienceWeb.com
POWERED BY SCIENCE DIRECT®

Neural Networks 16 (2003) 321–334

Neural Networks

www.elsevier.com/locate/neunet

2003 Special Issue

# Some neural network applications in environmental sciences. Part I: forward and inverse problems in geophysical remote measurements

Vladimir M. Krasnopolsky[a,*], Helmut Schiller[b]

[a]*Science Applications International Corporation at National Centers for Environmental Prediction, 5200 Auth Road, NWS/NOAA, Camp Spring, MD 20746, USA*
[b]*GKSS Research Center, Geesthacht, Germany*

**Abstract**

A broad class of neural network (NN) applications dealing with the remote measurements of geophysical (physical, chemical, and biological) parameters of the oceans, atmosphere, and land surface is presented. In order to infer these parameters from remote sensing (RS) measurements, standard retrieval and variational techniques are applied. Both techniques require a data converter (transfer function or forward model) to convert satellite measurements into geophysical parameters or vice versa. In many cases, the transfer function and the forward model can be represented as a continuous nonlinear mapping. Because the NN technique is a generic technique for nonlinear mapping, it can be used beneficially for modeling transfer functions and forward models. These applications are introduced in a broader framework of solving forward and inverse problems in RS. In this broader context, we show that NN is an appropriate and efficient tool for solving forward and inverse problems in RS and for developing fast and accurate forward models and accurate and robust retrieval algorithms. Theoretical considerations are illustrated by several real-life examples—operational NN applications developed by the authors for SSM/I and medium resolution imaging spectrometer sensors.


*Keywords:* Neural network; Remote sensing; Numerical weather prediction; Model emulation; Inverse modeling; Scope check

## 1. Introduction

Estimating high quality geophysical parameters (information about physical, chemical, and biological properties of the oceans, atmosphere, and land surface) from remote (satellite, aircraft, etc.) measurements is a very important problem in geosciences such as meteorology, oceanography, climatology and environmental modeling and protection. Direct measurements for many parameters of interest, like vegetation moisture, phytoplankton concentration in the ocean, and aerosol concentration in the atmosphere, are in general not available. Even when in situ measurements are available, they are usually sparse (especially over the oceans) and located only at the level of the ground or the ocean surface. Often such measurements can be estimated from the effect, which they caused on the electromagnetic radiation measured by a remote sensor. Remote measurements allow obtaining spatially dense measurements all around the globe at and above the level of the ground and oceans surface. The remote measurements themselves are usually very accurate. The quality of geophysical parameters derived from these measurements varies significantly depending on the strength and uniqueness of the signal from the geophysical parameters and mathematical methods applied to extract these parameters, i.e. to solve forward and inverse remote sensing (RS) problems. Neural network (NN) technique is a very promising mathematical tool to solve forward and inverse problems in RS accurately. The number of NN RS applications increased steadily during the last decade. A great number of publications have been devoted to particular applications, and only a few general review papers have been published in this and related areas (Atkinson & Tatnall, 1997; Gardner & Dorling, 1998; Hsieh & Tang, 1998). These review papers served a good service in introducing NN techniques to the RS community. However, only three particular areas of NN applications are well represented in reviews: image processing, classifications, and predictions.

Here we discuss a broad class of NN applications for solving forward and inverse problems in RS in order to infer geophysical parameters from satellite data, i.e. to produce

* Corresponding author. Tel.: 1-301-763-8000 ext. 7262; fax: 1-301-763-8545.
*E-mail address:* vladimir.krasnopolsky@noaa.gov (V.M. Krasnopolsky).

0893-6080/03/$ - see front matter © 2003 Elsevier Science Ltd. All rights reserved.
doi:10.1016/S0893-6080(03)00027-3

so-called satellite retrievals. Many particular applications belonging to this class have been published. The NN technique was applied for inversion of a multiple scattering model to estimate snow parameters from passive microwave measurements (Tsang et al., 1992). Smith (1993) used NNs for inversion of a simple two-stream radiative transfer model to derive the leaf area index from Moderate Resolution Imaging Spectrometer data. NNs were applied to simulate scatterometer measurements and to retrieve wind speed and direction from these measurements (Thiria, Mejia, Badran, & Crepon, 1993; Cornford, Nabney, & Ramage, 2001), to develop an inversion algorithm for radar scattering from vegetation canopies (Pierce, Sarabandi, & Ulaby et al., 1994), to estimate atmospheric humidity profiles (Cabrera-Mercader & Staelin, 1995), atmospheric temperature profiles (Aires et al., 2002), and atmospheric ozone profiles (Mueller et al., 2003). Stogryn, Butler, and Bartolac (1994), Krasnopolsky, Breaker, and Gemmill (1995) and Krasnopolsky, Gemmill, and Breaker (1995) applied NNs to invert Special Sensor Microwave Imager (SSM/I) data and to retrieve surface wind speed. Davis et al. (1995) applied NN for inversion of a forward model to estimate soil moisture, surface air temperature, and vegetation moisture from Scanning Multichannel Microwave Radiometer data. Using a NN technique, a fast SSM/I forward model (Krasnopolsky, 1997) and SSM/I multiparameter retrieval algorithm (Krasnopolsky, Breaker, & Gemmill, 1999, 2000) have been derived from empirical data (buoy SSM/I collocations). Abdelgadir et al. (1998) applied NNs for forward and inverse modeling of canopy directional reflectance. Schiller and Doerffer (1999) used a NN technique for inverting a radiative transfer forward model to estimate the concentration of phytoplankton pigment from Medium Resolution Imaging Spectrometer (MERIS).

In Section 2 of this paper we introduce and compare standard and variational retrieval techniques. Section 3 discusses NN applications in satellite RS. It is shown that both the forward model and the retrieval problem can be considered as nonlinear mappings and, therefore, can be approximated by NNs. In Sections 4 and 5 we introduce real-life examples of NN applications for SSM/I and MERIS sensors in order to show that NN can be used to optimize both retrieval algorithms and forward models. Section 6 contains conclusions and discussions, and Appendixes A and B present brief descriptions of the SSM/I and MERIS sensors.

## 2. Deriving geophysical parameters from satellite measurements: standard retrievals and variational retrievals through direct assimilation

Satellite RS data are used by a wide variety of users. Satellite sensors generate measurements in terms of radiances, backscatter coefficients, brightness temperatures, etc. The users of satellite data usually work with geophysical parameters such as pressure, temperature, wind speed and direction, water vapor concentration, etc. Satellite forward models, which emulate satellite measurements from given geophysical parameters, and retrieval algorithms, which transform satellite measurements into geophysical parameters, play the role of mediators between satellite sensors and users (Fig. 1). There exists an entire spectrum of different approaches in extracting geophysical information from the satellite measurements. At one end of this spectrum ‘satellite only’ approaches are located; we will call them standard or traditional retrievals. They use only measurements performed by one particular sensor, sometimes from different channels (frequencies, polarizations, etc.) of the same sensor, to estimate geophysical parameters. At the other end of the spectrum variational retrieval techniques (or direct assimilation techniques) are located. They use an entire data assimilation system, including numerical weather prediction (NWP) model and analysis (Prigent et al., 1997), which, in its turn, includes all kind of meteorological measurements (buoys, radiosondes, ships, aircrafts, etc.) as well as data from different satellite sensors. Many approaches have been developed which belong to the intermediate part of this spectrum. These approaches use measurements from several satellite sensors, combine satellite measurements with other kinds of measurements, and/or use background fields or profiles from NWP models for regularization of the inverse problem or for ambiguity removal, i.e. these approaches use some types of data fusion to regularize the solution of the inverse problem.

Fig. 1 shows the satellite data flow from instruments to users. Conventional methods for using satellite data (standard retrievals) involve solving an inverse (or retrieval) problem and deriving a transfer function (TF), $f$, which relates a geophysical parameter of interest, $G$ (e.g. surface wind speed over the ocean, atmospheric moisture concentration, sea surface temperature (SST), etc.) to a satellite measurement, $S$ (e.g. brightness temperatures, radiances, reflection coefficients, etc.)

$$G \underset{+}{\mathbf{f}} S \qquad 1$$

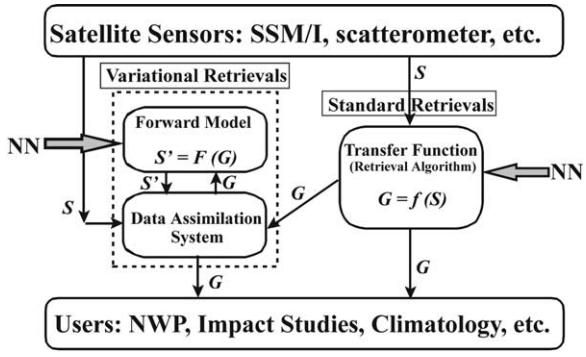


Fig. 1. Satellite measurement-to-user life cycle. Data processing converters (FM and TF), which can be optimized using NNs, are shown.

where both $G$ and $S$ may be vectors. The TF, $\mathbf{f}$, (it is also called a retrieval algorithm) usually cannot be derived directly from the first principles because the relationship (1) does not correspond to a cause and effect principle, and sometimes multiple values of $G$ can correspond to a single $S$. The inverse relationship, however, can be written

$$S \quad \mathbf{F}\ G \tag{2}$$

where $F$ is a forward model (FM), which relates a vector $G$ to a vector $S$. Forward models can usually be derived from physical considerations (e.g. radiative transfer theory) in accordance with the cause and effect principles because geophysical parameters affect the satellite measurements (not vice versa). Thus, the forward problem (2) is a well-posed problem in contrast to the inverse problem (1) which is often an ill-posed one (Parker, 1994); although, from the mathematical point of view, FM (2) and TF (1) both are continuous (or almost continuous) mappings between the two vectors $S$ and $G$. Even in the cases when the mapping (1) is not unique, this multi-valued mapping may be considered as a collection of single-valued continuous mappings.

In order to derive the TF (1), the FM (2) has to be inverted (an inverse problem has to be solved). The usually applied inversion technique searches for a vector $G^0$ which minimizes the functional (Stoffelen & Anderson, 1997)

$$\|\Delta S\| \quad \|S^0 - \mathbf{F}\ G\| \tag{3}$$

where $S^0$ is an actual vector of satellite measurements. Since the FM $\mathbf{F}$ is usually a complicated nonlinear function, this approach leads numerically to a full-scale nonlinear optimization with all its problems (slow convergence, multiple solutions etc). This approach does not determine the TF explicitly; it assumes this function implicitly, and for each new measurement $S^0$ the entire process has to be repeated. A simplified linearization method to minimize the functional (3) can be applied if one has a good approximation for the solution of the inverse problem, an approximate vector of geophysical parameters $G^0$. Then the difference vector $\Delta S$ is small and there is a vector $G$ in close proximity of $G^0$ ($|\Delta G| \quad |G - G^0|$ is small) where $\Delta S\ G \quad 0$. Expanding $\mathbf{F}\ G$ in a Taylor series and keeping only terms which are linear with respect to $\Delta G$, we can get a system of linear equations to calculate the components of the vector $\Delta G$ (Wentz, 1997)

$$\sum_{i\ 1}^{n} \frac{\partial \mathbf{F}\ G}{\partial G_i}\bigg|_{G\ G^0} \Delta G_i \quad S^0 - \mathbf{F}\ G^0 \tag{4}$$

where $n$ is the dimension of vector $G$. After $\Delta G$ is calculated, the next iteration of Eq. (4) with $G^0 \quad G^0 \quad \Delta G$ is performed. The process is expected to converge quickly to the vector of retrievals $G$. In this case again, the TF, $\mathbf{f}$, (1) is not determined explicitly, it is only determined implicitly for vector $S^0$ by the solution of Eq. (4). This type of retrievals can be called 'local' or 'localized' linear inversion. These techniques (Eq. (3) and (4)) are usually called physically based retrievals. It is important to emphasize that the physically based algorithms (Eq. (3) and (4)), by definition, are multi-parameter algorithms since they retrieve several geophysical parameters simultaneously (complete vector $G$ .

Empirical algorithms are based on an approach, which from the beginning, assumes the existence of an explicit analytical representation for a TF, $\mathbf{f}$. A mathematical (statistical) model, $\mathbf{f}_{\text{mod}}$, is usually chosen (usually some kind of regression) which contains a vector of empirical (or model) parameters $a \quad \{a_1, a_2, \ldots\}$,

$$G_k \quad \mathbf{f}_{\text{mod}}\ S, a \tag{5}$$

where these parameters are determined from an empirical (or simulated) matchup data set $\{G_k, S\}$ using, for example, statistical techniques such as the method of least-squares. This type of retrievals can also be called 'global' inversion as it is not restricted to a given vector of satellite measurements. The subscript $k$ in $G_k$ stresses the fact that the majority of empirical retrieval algorithms are single-parameter algorithms. For example, for SSM/I algorithms exist, which retrieve only wind speed (Goodberlet, 1989), or only water vapor (Alishouse, 1990; Petty, 1993), or cloud liquid water (Weng & Grody, 1994), etc. Krasnopolsky et al. (1999, 2000) showed that single-parameter algorithms have additional (as compared to multi-parameter retrievals) systematic (bias) and random (unaccounted variance) errors in a single retrieved parameter $G_k$.

The obvious way to improve single-parameter retrievals (5) is to include the other parameters in the retrieval process, using the empirical multi-parameter approach which, as in the physically based multi-parameter approach (3–4), inverts the data in the complete space of geophysical parameters. Thus, the complete vector of related geophysical parameters is retrieved simultaneously from a given vector of satellite measurements $S$

$$G \quad \mathbf{f}_{\text{mod}}\ S \tag{6}$$

Where $G \quad \{G_i\}$ is now a vector which contains the primary, physically-related, geophysical parameters, which contribute to the observed satellite measurements $S$. These retrievals do not contain the additional systematic and random errors just described. Because Eqs. (1), (2), (5), and (6) represent continuous mappings, the NN technique is well suited for emulating FM, TF and empirical TF, $\mathbf{f}_{\text{mod}}$.

Retrievals derived using a TF (1) are usually called standard retrievals. Standard retrievals have the same spatial resolution as the sensor measurements and produce instantaneous values of geophysical parameters over the areas where the measurements are available. Geophysical parameters derived using standard retrievals can be used for many applications such as the NWP data assimilation systems. In this case, a contribution to the variational

analysis cost function $\chi_G$ from a particular retrieval, $G^0$, is

$$\chi_G + \frac{1}{2} G - G^0 \; {}^{\mathrm{T}} O \quad E^{-1} G - G^0 \qquad 7$$

where $G^0 \quad \mathbf{f} S^0$ is a vector of retrieved geophysical parameter, $+S^0$ is a vector of sensor measurements, $G$ is a vector of geophysical parameters being analyzed, $O$ is the expected error covariance of the observations and $E$ is the expected error covariance of the retrieval algorithm.

Because standard retrievals are based on solution of inverse problem, which is usually mathematically ill-posed (Parker, 1994), this approach has some rather subtle properties and error characteristics (Eyre & Lorenc, 1989), which cause additional errors and problems in retrievals (e.g. amplification of errors, ambiguities, etc). As a result, high-quality sensor measurements might be converted into lower-quality geophysical parameters. This type of error can be avoided or reduced by using variational retrieval technique (or inversion) through direct assimilation of satellite measurements (Derber, 1992; Derber & Wu, 1998; Lorenc, 1986; Parrish & Phalippou, 1996; Prigent, Phalippou, & English, 1997).

Variational retrievals or direct assimilation of satellite data offer another way of deriving geophysical parameters from the satellite measurements (Fig. 1). Here, due to direct assimilation of sensor measurements, the entire data assimilation system is used for inversion (as a retrieval algorithm). In this case, a contribution to the analysis cost function $\chi_S$ from a particular sensor measurement, $S^0$, is

$$\chi_S + \frac{1}{2} S - S^0 \; {}^{\mathrm{T}} O \quad E^{-1} S - S^0 \qquad 8$$

where $S \quad \mathbf{F} G$, and $\mathbf{F}$ is a FM (2), which relates an analysis state vector $G$ (or vector of geophysical parameters in analysis) to a vector of simulated sensor measurements, $S$, $O$ is the expected error covariance of the observations, and $E$ is the expected error covariance of the forward model. The forward problem (2) is a well-posed problem in contrast to the inverse problem (1). However, a background term has to be added to Eq. (8) to prevent the data assimilation problem from being ill-posed (Parrish & Derber, 1992).

The retrieval in this case results in an entire field (global in the case of the global data assimilation system) for the geophysical parameter $G$ (retrievals are nonlocal) which has the same resolution as the numerical model used in the data assimilation system. This resolution may be lower or higher than the resolution of standard retrievals. The variational retrievals are also not instantaneous but usually averaged in time over the analysis cycle; however, the field is continuous and coherent (e.g. it should not have problems such as a directional ambiguity). The variational retrievals are the result of fusing many different types of data (including satellite data, ground observations, and numerical model first guess) inside the data assimilation system. Sparse standard retrievals can be converted into continuous fields, using regular data assimilation procedure (7). Retrieval technique (3) and its linearized version (4), which do not use and do not produce explicit TFs, are technically very close to variational retrievals; however, we will reserve this name for the type of retrieval technique which perform a direct assimilation of satellite data described above.

It is important to emphasize a very significant difference between the usage of the explicit TF for standard retrievals and the FM in variational retrievals. In standard retrievals the explicit TF (1) is usually simple (e.g. regression) and is applied once per sensor observation to produce a geophysical retrieval. In variational retrievals the FM, which is usually much more complicated than a simple explicit TF, and its partial derivatives (the number of derivatives is equal to $m \times n$, where $m$ and $n$ are the dimensions of the vectors $G$ and $S$, respectively), have to be estimated for each of the $k$ iterations performed during minimization of the cost function (8). Thus the requirements for simplicity of the FM used in the variational retrievals are restrictive, and variational retrievals often require some special, simplified and fast versions of FMs.

From the above discussion it is clear that standard retrievals of geophysical parameters and variational retrieval through direct assimilation of sensor measurements are complementary approaches, they often have different spatial and temporal resolutions, error properties, and they are oriented to different users and to different applications.

## 3. Forward and inverse problems in remote sensing and NNs

In principle, NNs can be used to emulate FMs (2) and TFs (1) because FM and TF both are continuous mappings. There are many practical advantages (computational speed, accuracy, robustness) that can be achieved by using NNs for emulating FMs and TFs. A further advantage is the easiness and flexibility of incorporating into the NN any additional geophysical parameter known to influence the satellite measurements but not appearing in the original FM and other additional information. This can improve the accuracy of the FM and can also help to regularize the inverse problem (Aires et al., 2002).

### *3.1. NNs for emulating forward models*

FMs are usually complex due to the complexity of the physical processes which they describe and due to the physical theories they are based on (e.g. radiative transfer theory). Dependencies of satellite measurements on geophysical parameters, which FMs describe, are complicated and nonlinear. Dependencies on different parameters may exhibit different types of nonlinear behavior. FMs are usually exploited in physically based retrieval algorithms where they are numerically inverted to retrieve geophysical parameters and in data assimilation systems, where they are

used for direct assimilation of satellite measurements (variational retrievals). Both, numerical inversion and direct assimilation are iterative processes, where FMs and their Jacobian are calculated many times for each satellite measurement. Thus, the retrieval process becomes very time consuming, sometimes prohibitively expensive for operational (real time) applications. For such applications it is essential to have fast and accurate versions of FMs. NNs can provide us with such fast and accurate FMs because NNs are fast, accurate and robust (Kerlirzin & Réfrégier, 1995) generic tools for modeling multiple nonlinear dependencies (continuous mappings) (Attali et al., 1997; Chen & Chen, 1995a,b; Cybenko, 1989; Funachashi, 1989; Hornik, 1991). Moreover, a NN also provides an entire Jacobian matrix with practically no additional computational efforts.

To develop a NN which approximates a FM, a training set which consists of matched pairs of vectors of geophysical parameters and satellite measurements, $\{G, S\}_{i\ 1,\ldots,N}$ has to be created. If a physically based FM exists, it can be used to generate the training set. Otherwise empirical data can be used to create a training set.

### 3.2. NNs for solving inverse problems (emulating retrieval algorithms)

For retrieval algorithms NNs can be used in several different setups. In physically based retrieval algorithms a NN, emulating the complex and slow physically based FM and its Jacobian, can be used to speed up local inversion process. In many cases NNs can be used for global inversion to explicitly invert a FM. In such cases, after inversion, the NN provides an explicit retrieval algorithm (or TF), which is a solution of the inverse problem and can be used for retrievals. To train NN, which emulates an explicit retrieval algorithm, a training set, $\{G, S\}_{i\ 1,\ldots,N}$, is required. As in the case of FMs, simulated or empirical data can be used to create the training set.

In addition to complications related to FMs (complexity, nonlinearity, etc.), retrieval algorithms exhibit additional problems because they are solutions of the inverse problem, which is an ill-posed problem. This is why mathematical tools, which are used to develop retrieval algorithms, have to be accurate and robust in order to deal with these additional problems. NNs are fast, accurate and robust tools for nonlinear (continuous) mappings and can be effectively used for modeling multi-parameter retrieval algorithms.

### 3.3. Controlling the NN generalization

NN are well suited to model complicated nonlinear relationships between multiple variables as it is the case in multispectral RS. Well-constructed NNs have good interpolation properties; however, they may produce unpredictable outputs when forced to extrapolate. The NN training data (produced by a FM or constructed from empirical data collections) cover a certain manifold $\mathbf{S}_T$ (a subspace $\mathbf{S}_T \in \mathbf{S}$ in the full $\mathbf{S}$ space. Real data to be fed into the NN $\mathbf{f}_{NN}$, which emulates a TF (1), may not always lie in $\mathbf{S}_T$. There are many sources for such deviations of real data from the low dimensional manifold $\mathbf{S}_T$ of simulated data, e.g. simplifications made in the construction of the model, neglecting the natural variability of parameters occurring in the model and measurement errors in the satellite signal not taken into account during the generation of the training data. When empirical data are used, extreme events (highest and lowest values of geophysical parameters) are usually not sufficiently represented in the training set because they have a low frequency of occurrence in nature. That means that in the retrieval stage real data in some cases may force the NN $\mathbf{f}_{NN}$ to extrapolate. The error resulting from such forced extrapolation will increase with the distance of the input point from $\mathbf{S}_T$ and will also depend on the orientation of the input point relative to $\mathbf{S}_T$.

Several actions can be taken in order to mitigate this problem. First, to ensure that the training data for a NN covers those domains of the NN input space which will be covered later by the measured data in the application stage, it is worth the effort to build in the variability of parameters into the training data by appropriate sampling during the forward model run generating the training data. Also the measurement errors should be added according to their probability distribution (if the covariance of the errors is not known, uncorrelated errors should be added). NNs to be trained with such data will possibly need more neurons and/or layers due to the need of mapping a now larger domain covering also larger ranges. Also the NN output error observed in the training as well as in the testing will be larger. But the NN will perform better in the operational phase. Another aspect to be considered before generating the NN training data is how to distribute the input variables of the FM: regions which need higher accuracy of inversion should be sampled more densely than less important ones. Unfortunately, when empirical data are used for NN training, the density, sampling and errors cannot be adjusted; they are given. In this case, a combination of empirical and simulated data may be helpful.

In order to recognize NN input not foreseen in the NN training phase and thus out of scope of the inversion algorithm, the validity check (Schiller & Krasnopolsky, 2001) can be used. Let the model $S = \mathbf{F}(G)$ have an inverse, $G = \mathbf{f}(S)$, then, by definition, $S = \mathbf{F}(\mathbf{f}(S))$. Further, let $\mathbf{f}_{NN}$ be the NN emulating the inverse model in the domain $\mathbf{S}_T$. The result of $G_0 = \mathbf{f}_{NN}(S_0)$ for $S_0 \notin \mathbf{S}_T$ may be arbitrary, and in general, $\mathbf{F}(\mathbf{f}_{NN}(S_0))$ will not be equal to $S_0$. The validity of $S = \mathbf{F}(\mathbf{f}_{NN}(S))$ is a necessary condition for $S \in \mathbf{S}$. Now, if in the application stage of the NN, $\mathbf{f}_{NN}$, $S$ is not in domain $\mathbf{S}_T$, the NN, $\mathbf{f}_{NN}$, is forced to extrapolate. In such a situation the validity condition may not be fulfilled, and the resulting $G$ in general is meaningless. For operational applications it is necessary to signal such events to the next higher evaluation level. In order to perform the validity test

the FM must be applied after each inversion. This requires a fast but accurate FM. Such FM can be achieved by a NN emulating accurately the original FM, $\mathbf{S} = \mathbf{F}_{NN}(G)$. So, the validity check algorithm consists of a combination of inverse and forward NNs that, in addition to the inversion, computes a quality measure for the inversion

$$\delta = \| S - \mathbf{F}_{NN}(\mathbf{f}_{NN}(S)) \| \quad (9)$$

In conclusion, the solution to the problem of scope check is obtained by verifying the retrieved parameters using a NN emulating the FM and comparing the result with the measurement. This procedure (i) allows the detection of situations where the forward model or/and transfer function is inappropriate, (ii) does an 'in scope' check for the retrieved parameters even if the allowed region has a complicated geometry, (iii) can be adapted to all cases where a NN is used to emulate the inverse of an existing forward model.

## 4. Neural networks for SSM/I data

In previous sections we discussed theoretical possibilities and premises for using NNs for modeling TFs and FMs. In this section we illustrate these theoretical considerations using real-life applications of the NN approach to the SSM/I forward and retrieval problems. SSM/I is a well-established instrument (Appendix A) flying since 1987; many different retrieval algorithms and several forward models have been developed for this sensor; and several different databases are available for the algorithm development and validation. Many different techniques have been applied for the algorithm development. Therefore, for this instrument, we can present an extensive comparison of different methods and approaches. A raw buoy-SSM/I matchup database created by the Navy was used for the NN algorithm development, validation, and comparison. This database is quite representative with the exception of high latitude and high wind speed events. In order to improve this situation the training set was enriched by adding a matchup databases collected by high latitude European ocean weather ships MIKE and LIMA to the Navy database. Many filters have been applied to remove errors and noisy data (for a detailed discussion see Krasnopolsky, Gemmill, & Breaker, 1996, 1999; Krasnopolsky, 1997).

### 4.1. NN empirical FM for SSM/I

The empirical SSM/I FM represents the relationship between a vector of geophysical parameters $G$ and a vector of satellite brightness temperatures (BTs, Appendix A) $S$, where $S = \{T19V, T19H, T22V, T37V, T37H\}$, $G = \{W, V, L, T_s \text{ or SST}\}$. Four geophysical parameters are included in $G$ (wind speed, $W$, columnar water vapor, $V$, columnar liquid water, $L$, and SST) which are the main parameters influencing satellite BTs, and which were used as inputs in the physically based FMs of Petty and Katsaros (1992, 1994) and Wentz (1997) (Table 1). The NN, OMBFM1 (Krasnopolsky, 1997), which implements this SSM/I FM has four inputs, $\{W, V, L, \text{SST}\}$, one hidden layer with 12 neurons, five nonlinear BT outputs $\{T19V, T19H, T22V, T37V, T37H\}$ (here $TXXY$ means: $XX$-frequency in GHz, $Y$-polarization), and 20 auxiliary outputs which produce derivatives of the outputs with respect to the inputs. These derivatives, which are not trained but calculated, constitute the Jacobian matrix, $\mathbf{K} = \{\partial S_i/\partial G_j\}$, which emerges in the process of direct assimilation of the SSM/I BTs when the gradient of the SSM/I contribution to the cost function (8), $\chi_s$, is calculated. The cost function gradient can be written as (Parrish & Derber, 1992; Phalippou, 1996)

$$\nabla\chi_s = \mathbf{K}\,\mathbf{X}^{\mathrm{T}}\,\mathbf{O}\,\mathbf{E}^{-1}\,\mathbf{F}\,\mathbf{X} - \mathbf{T}^{\mathrm{O}}$$

Fig. 2 shows the OMBFM1 architecture. Since these auxiliary outputs (Jacobian matrix **K**) are not independent, we did not include them in the error function during the training, hence, only the standard outputs **S** are involved in the training process. Estimating NN FM and its derivatives

Table 1
Comparison of physically based radiative transfer and empirical NN forward models for clear and clear cloudy (in parentheses) weather conditions

| Author | Type | Inputs | BT RMS Error (K) | |
|---|---|---|---|---|
| | | | Vertical | Horizontal |
| Petty and Katsaros (1992) | PB | $W$, $V$, $L$, SST, *Theta*[a], *P0*,[b] *HWV*[c], *ZCLD*[d], $Ta$[e], $G$[f] | 1.9 (2.3) | 3.3 (4.3) |
| Wentz (1997) | PB | $W$, $V$, $L$, SST, *Theta*[a] | 2.3 (2.8) | 3.4 (5.1) |
| Krasnopolsky (1997) | NN, emp. | $W$, $V$, $L$, SST | 1.5 (1.7) | 3.0 (3.4) |

[a] *Theta*, incidence angle.
[b] P0, surface pressure.
[c] *HWV*, vapor scale height.
[d] *ZCLD*, cloud height.
[e] $T_a$, effective surface temperature.
[f] $G$, lapse rate.

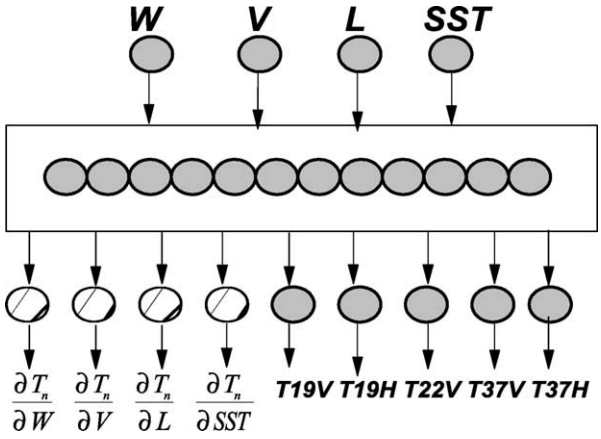


Fig. 2. NN forward model OMBFM1.

is a much simpler and faster task than calculating radiative transfer forward models.

The matchup databases for the F11 SSM/I have been used for training (about 3500 matchups) and testing (about 3500 matchups) our forward model. The FM was trained on all matchups which correspond to clear and cloudy weather conditions in accordance with the retrieval flags introduced by Stogryn et al. (1994). Only cases when the microwave radiation cannot penetrate the clouds were removed. Then, more than 6000 matchups for the F10 instrument have been used for validation and comparison of the NN FM with PB forward models by Petty and Katsaros (P&K) and Wentz (1997). The standard deviations (SDs) for OMBFM1 are systematically better than those for the P&K and Wentz FMs for all weather conditions and for all channels considered. For OMBFM1, the horizontally polarized channels, 19 and 37 H, have the highest SDs: ~2.5 K under clear, and ~3 K under clear and cloudy conditions. For the vertically polarized channels, SDs are lower: ≤1.5 K under clear, and ≤1.7 K under clear and cloudy conditions. The same trend can be observed for the P&K and Wentz FMs. Table 1 presents total statistics (RMS errors) for the three FMs discussed here. RMS errors are averaged over different frequencies for the vertical and horizontal polarization separately.

In this section we have demonstrated that the NN FM gives results which are comparable or better (in terms of RMS errors) than results obtained with more sophisticated physically based models. The NN FM simultaneously calculates the BTs and Jacobian matrix. It is much simpler than physically based FMs. The NN FM is not as general as radiative transfer models; it was developed for the usage in the data assimilation system for variational retrieval and direct assimilation of SSM/I BTs of particular frequencies from a particular instrument. However, for this particular application (direct assimilation) it has significant advantage (it is significantly faster), especially in an operational environment.

### 4.2. NN empirical SSM/I retrieval algorithms

The SSM/I wind speed retrieval problem is a perfect example to illustrate general statements formulated in previous sections. The problems encountered in the case of SSM/I wind speed retrievals and the methods used to solve them can be easily generalized for other geophysical parameters and sensors. About 10 different SSM/I wind speed retrieval algorithms, both empirical and physically based, have been developed using a large variety of approaches and methods. Here we perform a comparison of these algorithms in order to illustrate some properties of the different approaches mentioned in previous sections and some advantages of the NN approach.

Goodberlet, Swift, & Wilkerson, (1989) developed the first global SSM/I wind speed retrieval algorithm. This algorithm is a single-parameter algorithm (it retrieves only wind speed), and it is linear with respect to BTs (a linear multiple regression was used). Statistics for this algorithm are shown in Table 2 under abbreviation GSW. This algorithm presents a linear approximation of a nonlinear (especially under cloudy conditions) SSM/I TF, **f** (1). Under clear conditions (Table 2), it retrieves the wind speed with an acceptable accuracy (the SD is less than 2 m/s and the bias is low). However, under cloudy conditions where

Table 2
Error budget (in m/s) for different SSM/I wind speed algorithms for clear and clear cloudy (in parentheses) cases

| Algorithm | Method | Bias | Total RMSE | $W > 15$ m/s RMSE |
|---|---|---|---|---|
| GSW[a] | Multiple linear regression | −0.2 (−0.5) | 1.8 (2.1) | (2.7) |
| GSWP[b] | Generalized linear regression | −0.1 (−0.3) | 1.7 (1.9) | (2.6) |
| GS[c] | Nonlinear regression | 0.5 (0.7) | 1.8 (2.5) | (2.7) |
| Wentz[d] | Physically based | 0.1 (−0.1) | 1.7 (2.1) | (2.6) |
| OMBNN3[e] | NN | −0.1 (−0.2) | 1.5 (1.7) | (2.3) |

[a] Goodberlet et al. (1989).
[b] Petty (1993).
[c] Goodberlet and Swift (1992).
[d] Wentz (1997).
[e] Krasnopolsky et al., (1996, 1999).

the amount of the water vapor and/or cloud liquid water in the atmosphere increases, errors in the retrieved wind speed increase significantly (see Table 2, numbers in parentheses). This is because the TF, **f**, becomes essentially nonlinear. When the amount of the integrated water vapor in the atmosphere is significant (e.g. in tropics), the TF becomes nonlinear and the accuracy of GSW retrievals deteriorates significantly (Stogryn et al., 1994) even for clear conditions

Goodberlet and Swift (1992) tried to improve the performance of GSW algorithm under cloudy conditions, using nonlinear regression with a nonlinearity of rational type. Since the nature of the nonlinearity of the SSM/I TF under cloudy condition is not known precisely, an application of such a nonlinear regression with a particular fixed type of nonlinarity may not improve results. This is exactly what happens with this algorithm, which we refer to as GS. In many cases the GS algorithm generates false high wind speeds when real wind speeds are less than 15 m/s (Krasnopolsky et al., 1996).

A nonlinear (with respect to BTs) algorithm (GSWP) introduced by Petty (1993), and based on generalized linear regression, presents a case where a nonlinearity introduced in the algorithm represents the nonlinear behavior of TF much better. This algorithm introduces a nonlinear correction, which corrects the linear GSW algorithm when the amount of water vapor in the atmosphere is nonzero. Table 2 shows that GSWP algorithm improves the accuracy of retrievals as compared with the linear GSW algorithm under both clear and cloudy conditions. However, it does not improve performance of GSW algorithm at high wind speeds because most of the high wind speed events occur at mid- and high-latitudes, where the amount of the water vapor in the atmosphere is not significant. Here the cloud liquid water is the main source of the nonlinear behavior of the TF, and it has to be taken into account.

NN algorithms have been introduced as an alternative to the nonlinear and generalized linear regressions because the NN can model a nonlinear behavior of the TF better than these regressions. Stogryn et al. (1994) developed the first NN SSM/I wind speed algorithm, which consists of two NNs, one of them performs retrievals under clear and another one under cloudy conditions. Krasnopolsky, Gemmill, and Breaker (1994) and Krasnopolsky et al. (1995a,b) showed that a single NN with the same architecture can generate retrievals with the same accuracy as the two NNs developed by Stogryn et al. (1994) under both clear and cloudy conditions. This algorithm can be represented as

$$W_+ \quad \mathbf{f}_{\mathrm{NN}} \; S \qquad 10$$

where $W$ is the wind speed, and $S_+ \{T19V, T22V, T37V, T37H\}$. Application of Eq. (10) led to a significant improvement in wind speed retrieval accuracy for clear conditions. For higher moisture/cloudy conditions, the improvement was even greater (25–30%) compared to the GSW algorithm. The increase in the areal coverage due to improvements in accuracy was about 15% on average and higher in areas of significant weather.

Both NN algorithms give very similar results because they have been developed using the same matchup database. This database, however, does not contain matchups with wind speed higher than about 20 m/s and contains very few matchups with wind speeds higher than 15 m/s. These algorithms also are single-parameter algorithms, i.e. they retrieve only one parameter—wind speed; therefore, they cannot account for the variability of all related atmospheric (e.g. water vapor and liquid water) and surface (e.g. SST) parameters (especially important at higher wind speeds). This is why these NN algorithms pose the same problem; they cannot generate acceptable wind speeds at ranges higher then 18–19 m/s.

The next generation NN algorithm—a multi-parameter NN algorithm developed at NCEP (OMBNN3; Krasnopolsky et al., 1996, 1999) solved the high wind speed problem through three main advances. First, a new buoy/SSM/I matchup database containing an extensive matchup data set for F8, F10, and F11 sensors provided by NRL and augmented with additional data for high latitude, high wind speed events (up to 26 m/s) from European OWS MIKE and LIMA, was used for the development of this algorithm. Second, the method of NN training was improved by enhancing the learning of the high wind speed behavior. Third, the variability of related atmospheric and surface parameters was taken into account: wind speed, columnar water vapor, columnar liquid water, and SST are retrieved simultaneously. In this case, the relation (10) is modified

$$G_+ \quad \mathbf{f}_{\mathrm{NN}} \; S \qquad 11$$

where $G_+ \{W, V, L, \mathrm{SST}\}$ is now a vector, $W$ the wind speed, $V$ columnar water vapor, $L$ columnar liquid water, and SST is sea surface temperature. The OMBNN3 algorithm uses five SSM/I channels: 19 and 37 GHz (horizontal and vertical polarization) and 22 GHz (vertical polarization).

Fig. 3 illustrates the architecture of the OMBNN3 algorithm. Table 2 show a comparison of the performance

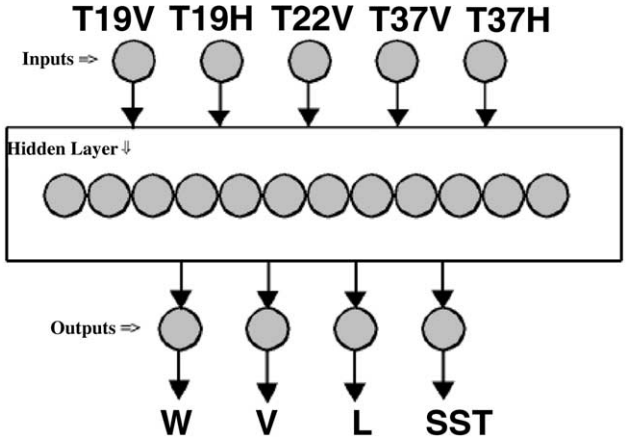


Fig. 3. The architecture of the OMBNN3 algorithm.

for all above-mentioned empirical algorithms. It also shows statistics for a physically based algorithm developed by Wentz (1997), which is based on linearized numerical inversion (4) of a physically based FM.

The statistics presented in Table 2 were calculated using about 15 000 of buoy-SSM/I matchups. The NN algorithm obviously outperforms all other algorithms. All algorithms, except the NN algorithms, show a tendency to overestimate high wind speeds. It happens because high wind speed events are usually accompanied by a significant amount of the cloud liquid water in the atmosphere. Under such circumstances, the transfer function, **f**, becomes a complicated nonlinear function and simple one-parametric regression algorithms cannot provide an adequate representation for this function and confuses a high concentration of cloud liquid water with very high wind speeds. OMBNN3 shows the best total performance (taking into account bias, RMSE, and high wind speed performance).

As was mentioned above, one of the significant advantages of OMBNN3 algorithms is its ability to retrieve simultaneously not only the wind speed but also three other atmospheric and ocean surface parameters: columnar water vapor $V$, columnar liquid water $L$, and SST. Krasnopolsky et al. (1996) showed that the accuracies of retrieval for $V$ and $L$ are very good and close to those for Alishouse et al. (1990) and Weng and Grody (1994) algorithms, respectively. However, the simultaneous and accurate retrievals of $V$ and $L$ is not the only advantage of OMBNN3.

Krasnopolsky et al. (1999, 2000) showed that the errors of OMBNN3 algorithm have weaker dependencies on related atmospheric ($V$ and $L$ and surface (SST) parameters than errors of other algorithms (single parameter algorithms) that have been considered. The retrieved SST in this case is not accurate (RMS error of about 4 °C; Krasnopolsky et al., 1996), however, including SST into the vector of retrieved parameters decreases the errors in other retrievals correlated with the SST.

### 4.3. Controlling the NN generalization in the SSM/I case

The OMBNN3 retrieval algorithm is running as the operational algorithm in the global data assimilation system at NCEP/NOAA since 1998. Given five brightness temperatures, it retrieves four geophysical parameters: ocean surface wind speed, water vapor and liquid water concentrations, and SST. At high levels of liquid water concentration the microwave radiation cannot penetrate clouds and surface wind speed retrievals become impossible.

Brightness temperatures for these occasions fall far outside the training domain $\mathbf{S}_T$. However, the retrieval algorithm in these cases, if not flagged properly, will produce wind speed retrievals, which are physically meaningless (i.e. not related to actual surface wind speed). Usually a statistically based retrieval flag is used to indicate such occurrences. Under complicated local conditions, however, this flag, because it is based on global statistics,

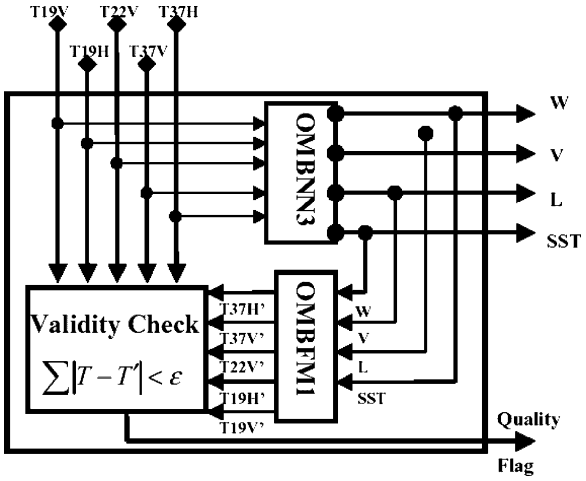


Fig. 4. SSM/I retrieval algorithm (OMBNN3) emulating the inverse model to retrieve vector $G$ of four geophysical parameters: ocean surface wind speed $W$, water vapor $V$ and liquid water $L$ concentrations, and SST if given five brightness temperatures $S^+$ $TXXY$ ($XX$-frequency in GHz, $Y$-polarization). This vector $G$ is fed to the OMBFM1 emulating the forward model to get brightness temperatures $S'$ $TXXY'$. The difference $\Delta S^+$ $|S-S'|$ is monitored and raises a warning flag if it is above a suitably chosen threshold.

produces significant amount of false alarms or does not produce alarms where needed. The validity check shown in Fig. 4, if added to standard retrieval flag, helps to indicate such occurrences. NN SSM/I forward model OMBFM1 is used in combination with the OMBNN3 retrieval algorithm. For each satellite measurement $S$, geophysical parameters retrieved from brightness temperatures $S$ are fed into NN SSM/I forward model, which produces another set of brightness temperatures $S'$. For $S$ within the training domain $S \in \mathbf{S}_T$) the difference, $\Delta S^+$ $|S-S'|$, is sufficiently small. For $S$ outside the training domain the difference raises a warning flag if it is above a suitably chosen threshold. Fig. 5a shows the percentage of removed data and improvements in the accuracy of the wind speed retrievals as functions of this threshold. Fig. 5b illustrates dependencies between the wind speed RMS error and maximum error and the percentage of the removed data. It shows that applying the generalization control reduces the RMS error significantly; the maximum error is reduced even more. It means that this approach is very efficient for removing outliers.

## 5. MERIS NN applications

This section presents a RS application for deriving the concentrations of water constituents from MERIS (the sensor is described to the extent necessary for understanding the discussion in Appendix B). The primary mission of MERIS is the measurement of sea color in the oceans and in coastal areas. The aim is to convert such measurements of the sea color into a measurement of concentrations of chlorophyll pigment, suspended sediment and gelbstoff

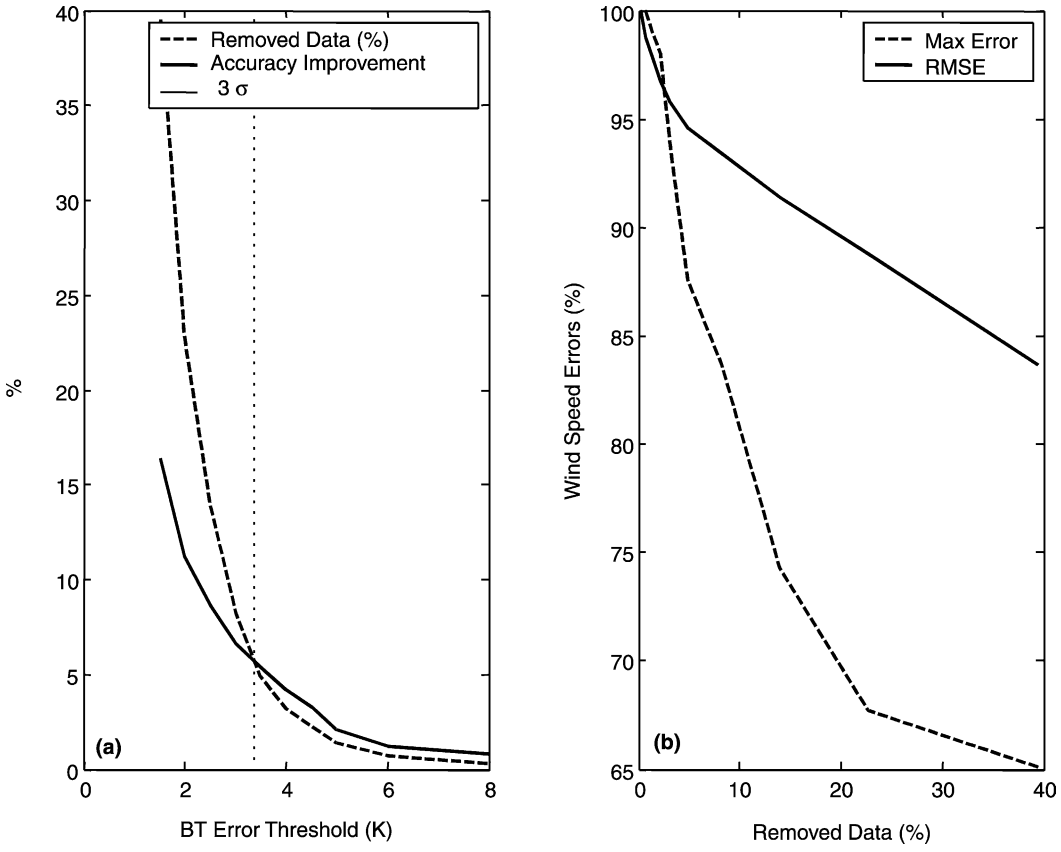


Fig. 5. (a) Percentage of removed data (dashed line) and wind speed accuracy improvement as functions of the threshold for BT discrepancy $\Delta S$. The vertical line shows three SDs for $\Delta S$. (b) Wind speed RMS and maximum errors dependency on the percentage of the removed data.

(dissolved organic material). The measurement of the ocean color relies on the measurement of the radiance of reflected sunlight in different spectral bands in the visible range arriving at the satellite. Most ($\geq 90\%$) of the light arriving at the satellite has been reflected by the atmosphere. Therefore, a careful atmospheric correction is necessary to calculate from the measured radiances the directional water leaving radiance reflectances (i.e. ocean color). The color of a given water mass depends on the viewing and illumination geometry, i.e. the zenith angles of sun and satellite and their azimuth difference. Therefore, the FM for this problem reads $r = \mathbf{F}(c, g)$ : the eight water leaving radiance reflectances $r$ depend on concentrations $c$ of water constituents and on three angles describing the geometry $g$ of the situation. The inverse model $c = \mathbf{f}(r, g)$ derives the concentrations of chlorophyll pigment, suspended sediment and gelbstoff.

For the ground-segment of MERIS, a retrieval procedure based on NN technology was developed to transform directional water leaving radiance reflectances measured in eight spectral bands and the three angles pixel by pixel with high efficiency into concentrations of the water constituents suspended matter, phytoplankton and gelbstoff. Additionally the NN checks if its input is in the domain, which was covered during the training of the NN.

Since measurements do not cover the data space with sufficient density, the construction of the NN is based on a large table (130 K entries) of simulated data generated by a Monte-Carlo radiative transfer code. For given concentrations of water constituents, the Monte-Carlo radiative transfer code calculates the angular distribution of water leaving radiance reflectance in eight visible MERIS bands. These angular distributions are sampled in the appropriate angle ranges to derive the entries of the training/test tables for building the NN: three concentrations, three angles and eight water leaving radiance reflectances. The sampling of the concentrations of the water constituents was done from an exponential distribution in order to disentangle small concentration differences in regions of small concentrations. In order to get roughly constant relative concentration errors the logarithm of the concentrations was used as NN output.

The natural variability of the inherent optical properties of the water constituents was built into the Monte-Carlo code by sampling the parameters describing the spectral dependence of the inherent optical quantities from their measured distributions. Also an error model was applied to the reflectances obtained in the Monte-Carlo run (until now only a theoretical error model is available from MERIS simulations).

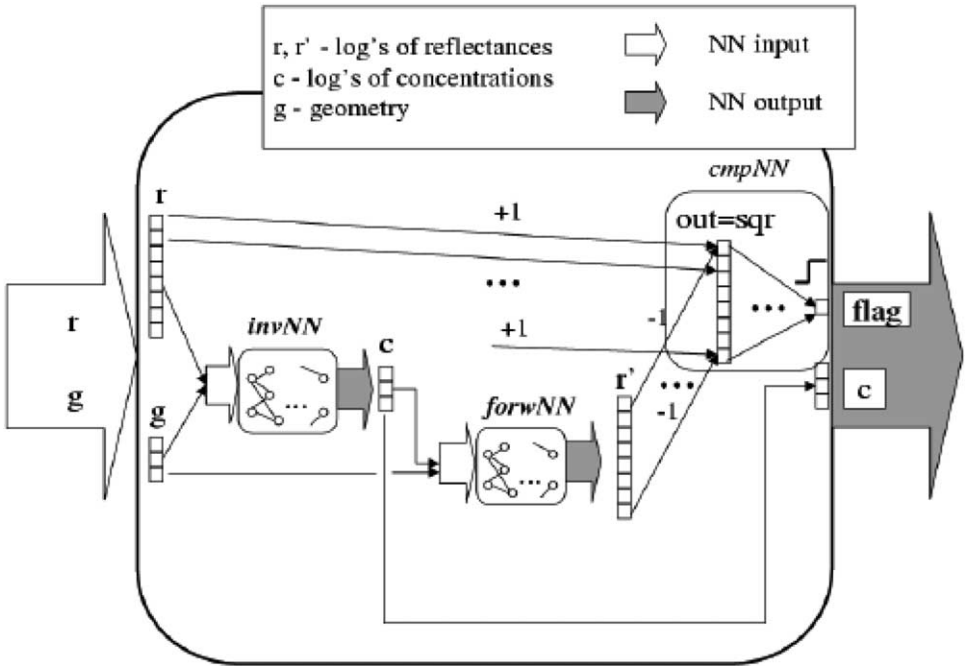


Fig. 6. Combined NNs applying quality check on water constituent concentrations retrieved from water leaving radiance reflectance measurements by MERIS.

Two NNs are trained with this table: (1) *inv*NN to emulate the inverse model or TF to derive concentrations $c$ from reflectances $r$ and geometry information $g$, and (2) *forw*NN to emulate the FM deriving reflectances $r$ from concentrations $c$ and geometry information $g$. The two NNs together with a comparison network are combined to give a new NN (Fig. 6), which first uses the *inv*NN part to obtain an estimate of the concentrations $c$. These are fed into the *forw*NN part, and the auxiliary NN component *cmp*NN compares the derived reflectances with the measured ones. Large deviations signal a violation of the necessary condition for a successful inversion; corresponding pixels are then flagged. Possible reasons for large deviations are (1) the atmospheric correction is bad, (2) the inherent optical properties of water constituent(s) could differ from those implemented in the bio-optical model, (3) the concentrations could be in a region not foreseen in the data base generation run, (4) foam or (5) nonconstant vertical profile. The restricted architecture of the MERIS processor only allows a single bit to specify the quality of the inversion. In less restricted cases one certainly will return the sum of the squared deviations.

The advantage of applying the error model to the training data is exemplified in Figs. 7 and 8. Two NNs were trained.

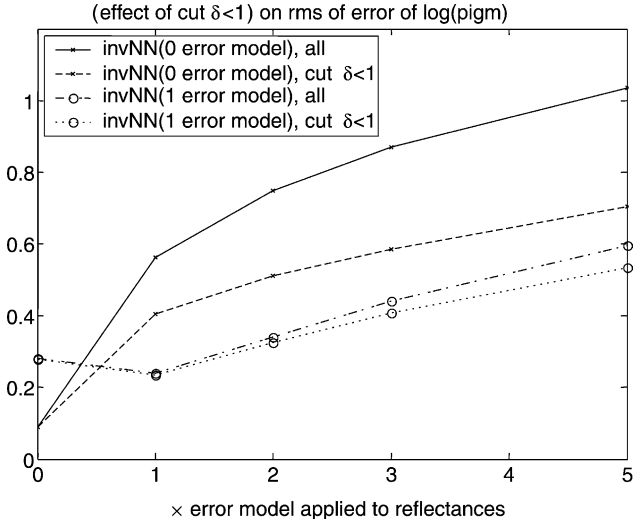


Fig. 7. NN output RMS error for *NN*0*err* and *NN*1*err* using input reflectances with varying amount of error. Results are shown without quality check (all) and with quality check (cut $\delta < 1$ , respectively.

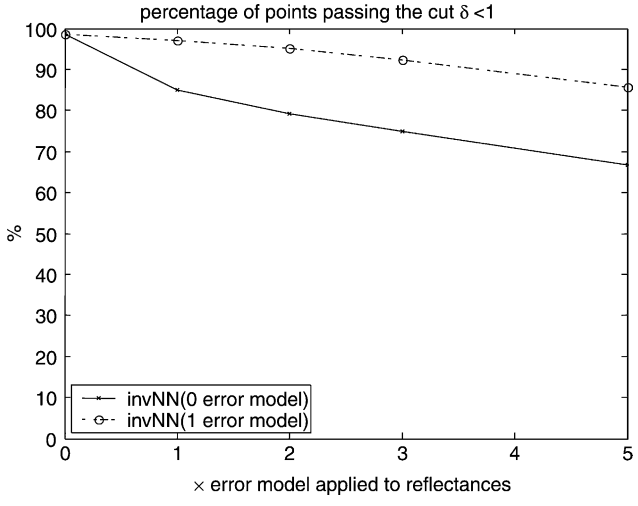


Fig. 8. Percentage of points passing the cut $\delta < 1$ for the two NNs *NN*0*err* and *NN*1*err* using input reflectances with varying amount of error.

The first NN *NN0err* was trained using the unmodified model output and the second NN *NN1err* was trained with the model output, which was modified by adding reflectance errors according to the error model. In Fig. 7 the RMS error of one of the NN outputs is plotted for both NNs for different input data sets. The input data sets differ in the amount of error added to the original model output. As expected, the *NN0err* performs better then *NN1err* when using input data from the original model. But for NN input with increasingly more error the *NN1err* outperforms *NN0err*.

The quality check (9) leads to a significant reduction of the NN output RMS error. In Fig. 8 the effect of the quality check $\delta < 1$ on the rate of accepted input is shown. For *NN0err* the acceptance of input points goes down rapidly, whereas for NN *NN1err* the acceptance of input is higher than 95% even if the input error is twice larger than expected. To improve the performance of the less robust NN *NN0err* much more input points must be rejected.

## 6. Conclusions

In this work we discussed a broad class of NN applications dealing with the solution of the RS forward and inverse problems. These applications are closely related to standard and variational retrievals, which estimate geophysical parameters from remote measurements. Both standard and variational techniques require a data converter to convert satellite measurements into geophysical parameters or vice versa. Standard retrievals use a TF (solution of the inverse problem) and variational retrievals use a FM (solution of the forward problem) for this purpose. In many cases the TF and the FM can be considered as a continuous nonlinear mapping. Because the NN technique is a generic technique for continuous nonlinear mapping it can be used beneficially for modeling TFs and FMs.

Theoretical considerations are illustrated by several real-life examples—operational NN applications developed by the authors for SSM/I and MERIS sensors. To illustrate benefits, which one can get from applying the NN approach to the FM and TF development, we have presented a new NN-based empirical SSM/I FM called OMBFM1 and a new NN-based OMBNN3 transfer function (i.e. retrieval algorithm) for SSM/I retrievals. Comparison with physically based FMs, for all weather conditions permitted, shows that OMBFM1 is better than or comparable with PB FMs in terms of accuracy. It is also significantly simpler than the PB FMs and much faster, which is very important for variational retrievals where the FM is estimated many times per satellite measurement. SSM/I NN applications have been developed using a significant amount of empirical data collected since the first sensor was launched in 1987.

The NN-based OMBNN3 transfer function (used as an operational algorithm at NCEP/NOAA since 1998) for SSM/I retrieves the wind speed, the columnar water vapor, the columnar liquid water, and the SST. It demonstrates high retrieval accuracy overall, together with the ability to retrieve high wind speeds with acceptable accuracy. The results demonstrate that OMBNN3 systematically outperforms all other statistically and physically based algorithms considered, under all weather conditions where retrievals are possible, and for all wind speeds.

The MERIS application presented in this paper shows a NN-based intelligent integral approach when the entire retrieval system, including the quality control block, is built as a combination of several specialized NNs. This approach offers significant advantages for real-life operational applications. This intelligent retrieval system not only produces accurate retrievals, it also performs an analysis and quality control of these retrievals and environmental conditions, rejecting poor retrievals if they occur. The MERIS NN application has been developed using a significant amount of simulated data.

The NN applications presented in this paper show the strengths and limits of the NN technique for derivation of environmental parameters from RS measurements. NNs successfully compete with other statistical methods and usually perform better than those because they are able to optimize the statistical link between the inputs and the outputs. NNs can successfully compete even with the physically based approaches because, in many cases, the explicit knowledge of very complicated physical processes in the environment is limited, and an NN-based empirical approach is more adequate. It can take into account more physics implicitly than a physically based approach can explicitly take into account. However, the success of the NN approach strongly depends on the training data set provided for the NN training. The availability, quality, representativeness, and size of this dataset are crucial for the success of the application.

## Acknowledgements

Authors thank D.B. Rao, W.H. Gemmill, and L.C. Breaker for their help and support in development of SSM/I NN applications and J. Derber for careful reviewing of this paper and constructive comments.

## Appendix A. The special sensor microwave imager (SSM/I)

Beginning in 1987, a series of special sensor microwave/imager (SSM/I) instruments have been launched through the defense meteorological satellite program (DMSP) (Hollinger, Lo, Poe, Savage, & Pierce, 1987). DMSP SSM/I satellites are polar orbiting satellites with a 102 min orbit. Each satellite provides coverage over a particular ocean basin twice a day, once during a descending orbit and once during an ascending orbit. The SSM/I

measures brightness temperatures in seven channels at four frequencies (19, 22, 37, and 85 GHz), each with vertical and horizontal polarization (22 GHz channel senses only vertical polarization). The spatial resolution is about 50 km at 19 and 22 GHz, about 30 km at 37 GHz and 15 km at 85 GHz. The SSM/I infers brightness temperatures from the ocean surface passively, receiving microwave radiation emitted by the ocean surface and passed through the atmosphere. The emission is effected by the surface wind speed (which changes the roughness of the ocean surface) and by the SST. The propagation of the microwave radiation through the atmosphere is influenced by the integrated amounts of water vapor and liquid water in the atmospheric column (Wentz, 1997, 1992). As a result the brightness temperatures carry signals from all these geophysical parameters and can then be converted into geophysical parameters (surface wind speed, columnar water vapor, columnar liquid water, and SST) using retrieval algorithms.

DMSP satellites have substantially increased the amount of real-time meteorological data that is acquired over the oceans. This data is used subjectively by marine meteorologists to improve ocean surface weather map analyses, and objectively by numerical analysis systems to provide initial conditions for NWP models. With three satellites in orbit and with a swath width of about 1400 km for each of the satellites, high-resolution coverage is now available almost globally on a daily basis. A significant amount of data has been collected and matched to the buoy data since 1987.

## Appendix B. The Medium resolution imaging spectrometer (MERIS)

In January 2002, the European Space Agency will launch Envisat, an advanced polar-orbiting Earth observation satellite that will provide measurements of the atmosphere, ocean, land and ice over a 5 year period. The Envisat satellite has an ambitious and innovative payload that will ensure the continuity of the data measurements of the ESA ERS satellites. The Envisat data will support Earth science research and allow monitoring of the evolution of environmental and climatic changes.

One of the instruments onboard Envisat will be MERIS (Rast, Beézy, & Bruzzi, 1999). The primary mission of MERIS is the measurement of sea color in the oceans and in coastal areas. Such measurements of the sea color, after atmospheric correction, can be converted into a measurement of concentrations of chlorophyll pigment, suspended sediment and gelbstoff (dissolved organic material). Main application domains of such data are (1) the ocean carbon cycle, (2) the thermal regime of the upper ocean and (3) the management of fisheries and of coastal zones. MERIS allows global coverage of the Earth in 3 days.

MERIS is an imaging spectrometer, which measures the solar reflected radiation from the Earth in the visible and near infrared part of the spectrum during daytime. The 1150 km wide swath is divided into five segments covered by five identical cameras having corresponding fields of view with a slight overlap between adjacent cameras. Each camera images an across-track stripe of the Earth's surface onto the entrance slit of an imaging optical grating spectrometer. This entrance slit is imaged through the spectrometer onto a two-dimensional CCD array, thus providing spatial and spectral information simultaneously. MERIS is designed to acquire 15 spectral bands in the 390–1040 nm range of the electromagnetic spectrum.

The spatial information along-track is determined via successive read-outs of the CCD-array. Full spatial resolution data, i.e. 300 m at nadir, will be transmitted over coastal zones and land surfaces. Reduced spatial resolution data, achieved by on board combination of $4 \times 4$ adjacent pixels across-track and along-track resulting in a resolution of approximately 1200 m at nadir, will be generated continuously.

## References


Abdelgadir, A., et al. (1998). Forward and inverse modeling of canopy directional reflectance using a neural network. *International Journal of Remote Sensing*, *19*, 453–471.

Aires, F., et al. (2002). A regularized neural net approach for retrieval of atmospheric and surface temperature with the IASI instrument. *Journal of Applied Meteorology*, *41*, 144–159.

Alishouse, J. C., et al. (1990). Determination of oceanic total precipitable water from the SSM/I. *IEEE Transactions on Geoscience and Remote Sensing, GE*, *23*, 811–816.

Atkinson, P. M., & Tatnall, A. R. L. (1997). Neural networks in remote sensing—introduction. *International Journal of Remote Sensing*, *18*(4), 699–709.

Attali, J.-G., & Pagés, G. (1997). Approximation of functions by a multilayer perceptron: a new approach. *Neural Networks*, *10*, 1069–1081.

Cabrera-Mercader, C. R., & Staelin, D. H. (1995). Passive microwave relative humidity retrievals using feedforward neural networks. *IEEE Transactions on Geoscience and Remote Sensing*, *33*, 1324–1328.

Chen, T., & Chen, H. (1995a). Approximation capability to functions of several variables, nonlinear functionals, and operators by radial basis function neural networks. *Neural Networks*, *6*, 904–910.

Chen, T., & Chen, H. (1995b). Universal approximation to nonlinear operators by neural networks with arbitrary activation function and its application to dynamical systems. *Neural Networks*, *6*, 911–917.

Cornford, D., Nabney, I. T., & Ramage, G. (2001). Improved neural network scatterometer forward models. *Journal of Geophysical Research*, *106*, 22331–22338.

Cybenko, G. (1989). Approximation by superposition of sigmoidal functions. *Mathematics of Control, Signals and Systems*, *2*, 303–314.

Davis, D. T., et al. (1995). Solving inverse problems by Bayesian iterative inversion of a forward model with application to parameter mapping using SMMR remote sensing data. *IEEE Transactions on Geoscience and Remote Sensing*, *33*, 1182–1193.

Derber, J. C., & Wu, W.-S. (1998). The use of TOVS cloud-cleared radiances in the NCEP SSI analysis system. *Monthly Weather Reviews*, *126*, 2287–2299.

Eyre, J. R., & Lorenc, A. C. (1989). Direct use of satellite sounding radiances in numerical weather prediction. *Meteorology Magazine*, *118*, 13–16.

Funahashi, K. (1989). On the approximate realization of continuous mappings by neural networks. *Neural Networks*, *2*, 183–192.

Gardner, M. W., & Dorling, S. R. (1998). Artificial neural networks (the multiplayer perceptron)—a review of applications in the atmospheric sciences. *Atmospheric Environment*, *32*, 2627–2636.

Goodberlet, M. A., Swift, C. T., & Wilkerson, J. C. (1989). Remote sensing of ocean surface winds with the special sensor microwave imager. *Journal of Geophysical Research*, *94*, 14547–14555.

Goodberlet, M. A., & Swift, C. T. (1992). Improved retrievals from the DMSP wind speed algorithm under adverse weather conditions. *IEEE Transactions on Geoscience and Remote Sensing*, *30*, 1076–1077.

Hollinger, J., Lo, R., Poe, G., Savage, R., & Pierce, J. (1987). *Special sensor microwave/imager user's guide* (*120*). *Technical report*, Washington, DC: Naval Research Lab.

Hsieh, W. W., & Tang, B. (1998). Applying neural network models to prediction and data analysis in meteorology and oceanography. *Bulletin of American Meteorological Society*, *79*, 1855–1870.

Hornik, K. (1991). Approximation capabilities of multilayer feedforward network. *Neural Networks*, *4*, 251–257.

Kerlirzin, P., & Réfrégier, P. (1995). Theoretical investigation of the robustness of multilayer perceptrons: analysis of the linear case and extension to nonlinear networks. *IEEE Transactions on neural networks*, *6*, 560–571.

Krasnopolsky, V. M., Breaker, L. C., Gemmill, W. H (1994). Development of a single all-weather neural network for estimating ocean surface winds from the special sensor microwave imager. Technical note, OPC contribution No. 94, NMC/NOAA.

Krasnopolsky, V., Breaker, L. C., & Gemmill, W. H. (1995a). A neural network as a nonlinear transfer function model for retrieving surface wind speeds from the special sensor microwave imager. *Journal of Geophysical Research*, *100*, 11033–11045.

Krasnopolsky, V., Gemmill, W. H., Breaker, L. C (1995). Improved SSM/I wind speed retrievals at high wind speeds. Technical note, OMB contribution No. 111, NCEP/NOAA. Washington, DC.

Krasnopolsky, V., Gemmill, W. H., Breaker, L. C (1996). A new transfer function for ssm/i based on an expanded neural network architecture. Technical note, OMB contribution No. 137, NCEP/NOAA.

Krasnopolsky, V (1997). A neural network-based forward model for direct assimilation of SSM/I brightness temperatures, Technical note, OMB contribution No. 140, NCEP/NOAA.

Krasnopolsky, V. M., Gemmill, W. H., & Breaker, L. C. (1999). A multi-parameter empirical ocean algorithm for SSM/I retrievals. *Canadian Journal of Remote Sensing*, *25*, 486–503.

Krasnopolsky, V. M., Gemmill, W. H., & Breaker, L. C. (2000). A neural network multi-parameter algorithm SSM/I ocean retrievals: comparisons and validations. *Remote Sensing of Environment*, *73*, 133–142.

Lorenc, A. C. (1986). Analysis methods for numerical weather prediction. *Quarterly Journal of Royal Meteorology Society*, *122*, 1177–1194.

McNally, A. P., Derber, J. C., Wu, W.-S., & Katz, B. B. (2000). The use of TOVS level 1B radiances in the NCEP SSI analysis system. *Quarterly Journal of Royal Meteorological Society*, *126*, 689–724.

Mueller, M. D. et al (2003). Ozone profile retrieval from GOME data using a neural network approach (NNORSY). *Journal of Geophysical Research*. To be published.

Parker, R. L. (1994). *Geophysical inverse theory*. Princeton: Princeton University Press.

Parrish, D. F., & Derber, J. C. (1992). The national meteorological center's spectral statistical-interpolation analysis system. *Monthly Weather Reviews*, *120*, 1747–1763.

Phalippou, L. (1996). Variational retrieval of humidity profile, wind speed and cloud liquid–water path with the SSM/I: potential for numerical weather prediction. *Quarterly Journal of Royal Meteorological Society*, 122327–122355.

Petty, G. W. (1993). A comparison of SSM/I algorithms for the estimation of surface wind. *Proceedings Shared Processing Network DMSP SSM/I Algorithm Symposium*, *8–10*(June), 1993.

Petty, G. W., & Katsaros, K. B. (1992). The response of the special sensor microwave/imager to the marine environment. Part I: an analytic model for the atmospheric component of observed brightness temperature. *Journal of Atmospheric Oceanic Technology*, *9*, 746–761.

Petty, G. W., & Katsaros, K. B. (1994). The response of the SSM/I to the marine environment. Part II: A parameterization of the effect of the sea surface slope distribution on emission and reflection. *Journal of Atmospheric Oceanic Technology*, *11*, 617–628.

Pierce, L., Sarabandi, K., & Ulaby, F. T. (1994). Application of an artificial neural network in canopy scattering inversion. *International Journal of Remote Sensing*, *15*, 3263–3270.

Prigent, C., Phalippou, L., & English, S. (1997). Variational inversion of the ssm/i observations during the ASTEX campaign. *Journal of Applied Meteorology*, *36*, 493–508.

Rast, M., Beézy, J. L., & Bruzzi, S. (1999). The ESI Medium Resolution Imaging Spectrometer MERIS—a review of the instrument and its mission. *International Journal of Remote Sensing*, *20*, 1735–1746. see also URL http://envisat.esa.int/instruments/meris/descr/charact.htm.

Schiller, H., & Doerffer, R. (1999). Neural network for emulation of an inverse model—operational derivation of case II water properties from MERIS data. *International Journal of Remote Sensing*, *20*, 1735–1746.

Schiller, H., Krasnopolsky, V. M (2001). Domain check for input to NN emulating an inverse model. *Proceedings of International Joint Conference on Neural Networks*, July 15–19, (pp. 2150–2152). Washington, DC.

Smith, J. A. (1993). LAI inversion using a back-propagation neural network trained with a multiple scattering model. *IEEE Transactions on Geoscience and Remote Sensing*, *GE-31*, 1102–1106.

Stoffelen, A., & Anderson, D. (1997). Scatterometer data interpretation: estimation and validation of the transfer function CMOD4. *Journal of Geophysical Research*, *102*, 5767–5780.

Stogryn, A. P., Butler, C. T., & Bartolac, T. J. (1994). Ocean surface wind retrievals from special sensor microwave imager data with neural networks. *Journal of Geophysical Research*, *90*, 981–984.

Thiria, S., Mejia, C., Badran, F., & Crepon, M. (1993). A neural network approach for modeling nonlinear transfer functions: application for wind retrieval from spaceborn scatterometer data. *Journal of Geophysical Research*, *98*, 22827–22841.

Tsang, L., et al. (1992). Inversion of snow parameters from passive microwave remote sensing measurements by a neural network trained with a multiple scattering model. *IEEE Transactions on Geoscience and Remote Sensing*, *GE-30*, 1015–1024.

Weng, F., & Grody, N. G. (1994). Retrieval of cloud liquid water using the special sensor microwave imager (SSM/I). *Journal of Geophysical Research*, *99*, 25535–25551.

Wentz, F. J. (1997). A well-calibrated ocean algorithm for special sensor microwave/imager. *Journal of Geophysical Research*, *102*, 8703–8718.